Early-age shrinkage and bond of LC-TRM strengthening in rammed earth

Rafael Ramírez Eudave [*], Rui A. Silva, Eduardo Pereira, Antonio Romanazzi

ISISE – Institute for Sustainability and Innovation in Structural Engineering, University of Minho, School of Engineering, Civil Engineering Department, Azurém Campus, 4800-058 Guimarães, Portugal

ARTICLE INFO

ABSTRACT

The wide dissemination of earth-based structures as contemporary, vernacular or heritage constructions in regions with important seismic hazard demands the design of solutions that improve the typical low structural performance resulting from intrinsic material limitations. Only in this way, it is possible to promote a comprehensive seismic protection of this heritage and of the life of their inhabitants. One relevant and innovative solution proposed recently to address this problem consists in the strengthening with low-cost textile meshes embedded in a mortar matrix (LC-TRM). The purpose of this solution is similar to that of fibre reinforced polymers (FRP) systems used in masonry structures, where it works as an externally bonded reinforcement. Nevertheless, LC-TRM is addressed to elements constituted by materials with low mechanical properties, such as rammed earth and adobe. The further development of this strengthening solution demands comprehending with detail the interaction between the substrate and the matrix, where the shrinkage behaviour is relevant for the success of the system. The capacity of non-destructive tests based on digital image correlation (DIC) suggest the possibility of using this technique to monitor mortar shrinkage in LC-TRM strengthened rammed earth walls. On this regard, an experimental program was conducted and provided many important conclusions, among which are that DIC provides an adequate monitoring of the shrinkage behaviour of LC-TRM strengthened systems and that the strengthening mesh is a key element for controlling shrinkage development. Additionally, the interaction between the substrate and the LC-TRM system was characterised by the means of pull-off tests, favouring a discussion on the suitability and limitations of these tests on rammed-earth/LC-TRM systems.

1. Introduction

Buildings made of raw earth are widely found all around the world, comprising a rich variety of chronologic stages in human history. This fact is a consequence of the multiple conveniences that earthen-based materials represent in terms of availability, easy utilisation and durability. Nowadays, earth architecture is still present in many housing solutions [1] as well as in numerous historical monuments. The United Nations Educational, Scientific and Cultural Organization (UNESCO) considers that 20 % of the cultural historical assets are related to earthen-based building techniques [2].

Earthen constructions, however, are sensitive to environmental elements, namely to the effect of superficial erosion due to wind and rain. This vulnerability forces the existence of periodic maintenance works focused on the application or restitution of coatings for protecting the core of the structural elements, namely walls [3]. Thus, such works became frequent in the conservation and protection of historical monuments. These coatings are traditionally applied with earth-based mortars and experience has evidenced that the addition of natural fibres enhances the behaviour of the coating by limiting its shrinkage deformation and, intrinsically, by permitting a better bond to the substrate [4].

The mechanical properties of earth-based materials define some of the constructive features of the structural elements composed with them. For instance, the typical low values lead to adopt relatively low slenderness ratios in walls. Thus, these elements present large thicknesses, which make them heavy weighted. The high self-weight of earthen walls conjugated with the typical very low tensile strength of the material make these buildings vulnerable when facing seismic actions. Besides these two properties inherent to earthen materials, the ineffective connections among structural elements also affect/increment the seismic vulnerability of earth-based constructions.[5]

On this regard, the addition of natural fibres in earthen materials is a traditional strategy used to increase the tensile strength of the structural elements [6]. In existing buildings, a similar approach can be used, where synthetic meshes can be embedded in a coating mortar

---

* Corresponding author.
E-mail addresses: r.92@outlook.es (R. Ramírez Eudave), ruisilva@civil.uminho.pt (R.A. Silva), eduardo.pereira@civil.uminho.pt (E. Pereira).

adequately bonded to the earthen element. To this purpose, low-cost meshes can be combined with earth-based mortars compatible with the earthen support. This strategy, previously explored in the works of Romanazzi et al. and Sadeghi et al. [7,8], is expected to result in economical structural enhancements with minimum intervention on historical buildings, while addressing durability concerns.

Rammed earth consists in a series of compacted layers of moistened earth that are subsequently overlayed within a formwork to build walls. Nowadays, this technique is becoming increasingly more appreciated for the physical and sustainability features of the material [9,10]. For instance, rammed earth has an incorporated energy by mass unit of approximately 0.02 MJ/kg against the more than 1.00 MJ/kg of Portland cement [11]. The few existing standards highlight the particle size distribution of the soil as one of the most important attributes defining the performance of rammed earth, which encompasses the proportions of the main fractions, namely: clay, silt, sand and gravel [12]. Table 1 presents the proportions ranges recommended by different authors, such as Duarte [13], Schroeder [14] and the Swiss Centre for Development Cooperation in Technology and Management (SKAT) [15].

The soil with adequate proportions between fractions is mixed with water to start compacting rammed earth, which is conducted by means of manual or mechanic rammers. In fact, the water content of the soil mixture is one of the most critical aspects for the quality of the material. The presence of water is important to lubricate the soil particles and facilitate the compaction. However, excessive contents prejudice the compaction efficiency (material with lower dry density) and may result in excessive volumetric reduction of the rammed earth due to drying, leading to relevant cracking. Some standards limit the maximum linear shrinkage between 0.05 % (New Zealand NZS 4298:1998 [17]) and 3.0 % (Scottish Executive norm [18]). The formwork is typically made of timber and defines the final geometry of the walls. It traditionally consists of a modular unit, which is reused to compact subsequent blocks, while it is supported directly on the wall. The block generally has a height of 40–70 cm, length of about 2 m and width of about 50–60 cm, while the thickness of the layers can be of about 10 cm [10].

The relatively modest mechanical properties of rammed earth have been traditionally improved with different approaches, mostly in contexts of intense seismic activity. For instance, embedding tensile-resistant materials, such as timber elements, allows the admission of a certain level of tensile stresses on the structure and facilitates the dissipation of energy [19]. Another interesting approach for existing buildings is the addition of timber elements in the interior and exterior surfaces of the walls, with connections across the thickness. The installation of these elements is normally done by operating ad hoc grooves that subsequently permit to apply a homogenous layer of plaster. This approach permits to enhance the ductility of the structure and presents a relatively low cost [20]. Another approach is centred on embedding reinforcing meshes in mortar coatings, forming a composite material bonded to the surface of the walls. This solution has numerous advantages, such as easy application, great durability and low intrusion regarding the original building [21]. It is a solution with growing application on concrete and masonry structures, where it is known as Textile Reinforced Mortars (TRM) or Fibre Reinforced Cementitious Mortar (FRCM). The mortar has the function of protecting the fibres and transmitting the stresses from the substrate (i.e., the rammed earth wall). Hence, the interaction between the substrate and the mortar is fundamental for the adequate performance of the system.

Experimental research has shown that masonry walls strengthened with TRM are able to develop between 4 and 31 times more ultimate strain than the unstrengthened ones, while the ultimate load capacity increases from 2 to 13 times [22]. It should be noted that the existence of a weak substrate combined with stiff TRM strengthening solutions specific for masonry may promote damage or detachments. Thus, the use of meshes with lower strength combined with compatible mortars has been explored to improve the mechanical compatibility between earthen substrates and the TRM system, as well as the affordability of the solution. Since this approach is focused on the use of low-cost materials, it was named as Low-Cost TRM or LC-TRM [7]. On this regard, the works of Barroso [23] and Romanazzi [24] have documented the impact that LC-TRM retrofitting has in the mechanical behaviour of rammed-earth structures.

The multiple alternatives for the mortar and the mesh open a wide set of potential combinations comparable in terms of compatibility and durability. Some authors [23] recommend the use of relatively plastic mortars for earthen substrata, which may result from combination of different proportions of raw materials, such as lime, sand, clay or cement. Earth-based mortars are known for their great compatibility with earthen supports [25], though they are vulnerable to degradation by environmental agents, which frequently leads to their stabilisation with lime or cement. The addition of these binders also changes other properties of the mortars. However, interventions using cement-based mortars are associated to severe incompatibility problems regarding their higher stiffness and lower porosity when compared to earthen substrata [26].

The shrinkage behaviour is also affected by the stabilisation of the earth-based mortar, which in turn is expected to affect the adhesion and durability of the LC-TRM strengthening. For instance, the surface of the rammed earth walls constrains the shrinkage of the mortar coating, meaning that the mortar should be able to accommodate curing/drying deformations without cracking or losing adhesion to the support. Thus, characterizing the early-age shrinkage behaviour of LC-TRM strengthening solutions is of utmost importance to assess their structural and durability performance.

This work proposes a method to monitor the early-age shrinkage of LC-TRM systems on rammed-earth walls, with the objective of characterising how different combinations of mortars and meshes interact with the substrate. To this purpose, the method should be able to measure the magnitude of shrinkage, as well as the potential for development of surface micro-cracking patterns. The paper starts by presenting the materials adopted in the experimental program, which includes different reinforcing meshes and coating mortars, as well as the material used to simulate rammed earth substrata. Then, a data-acquisition system based on photographic images is presented and implemented facilitating a time-dependent observation of changes in the mortar's surface during the first stages of drying. The outputs are presented and discussed, by comparing significative differences among the proposed LC-TRM configurations and by pointing out some potential opportunities and limitations of the proposed method. In addition, the specimens used in the experimental program were further explored for evaluating the bond strength of different LC-TRM configurations through pull-off tests. This set of experiments proposes an adapted version of standard procedures, permitting to discuss some limitations for testing LC-TRM solutions on rammed-earth substrates.

2. Characterising the shrinkage of mortars

The shrinkage of mortars may be influenced by a series of factors, such as environmental conditions, the interaction with substrate and type of mortar. Nevertheless, the main component of shrinkage for

Table 1
Proportions between soil fractions recommended for rammed earth construction.

Fraction	Diameter (mm) ISO 14688–1:2016 [16]	Recommended percentages		
		Duarte 2013 [13]	SKAT 1993 [15]	Schroeder 2016 [14]
Clay	<0.002	10–20 %	10–20 %	Min 20–25 %
Silt	0.002–0.063	20–35 %	15–30 %	Max 30–35 %
Sand	0.063–2.0	40–50 %	50–75 %	Min 50–55 %
Gravel	greater than 2.0	<15 %		Max 70–75 %

earth-based materials is drying, given the volumetric loss on clay particles when part of the water is lost by evaporation. Shrinkage on mortars with hydraulic binders combine this drying shrinkage with plastic, autogenous and carbonation shrinkage [5].

A typical approach for assessing the shrinkage of mortars for earthen buildings resorts to the Alcock test. On this regard, Barroso [23] presents an experimental program for measuring the linear shrinkage of earth-based mortars for rammed earth, considering the water content and the addition of sand in different proportions as variables. The specimens were prepared with dimensions $30 \times 30 \times 300$ mm^3 by casting the mortar in two layers in timber moulds, which had the internal surfaces covered with plastic film. Casting was preceded of lubrication of the moulds to mitigate friction and promote the free shrinkage of the specimens. The samples were stored in a climatic chamber during 28 days in controlled conditions of 20 ± 1 °C temperature and 60 ± 2 % relative humidity. The results evidenced an increase in shrinkage with increasing water content, while the addition of sand helped to control the shrinkage. Similar observations were previously presented in Ruzicka et al. [27] for a variety of earth mixtures (see Table 2).

On the other hand, the Alcock test has several limitations. In fact, it may not represent multiple factors that influence and constrain the shrinkage behaviour of mortar coatings. For instance, the interaction regarding the substrate, the exchange of water during the drying process and the two-dimensional in-plane effects. Therefore, an alternative method for measuring the superficial shrinkage of LC-TRM strengthening, based on Digital Image Correlation (DIC) technique, is here proposed. DIC is an optical contactless method that permits to compare a series of photographs taken with a determined frequency. Through finding the differences between them, it is possible to identify deformations with a precision of $\pm$ 0.01 pixels and strains of the order of $\pm 100\mu\varepsilon$. This method is based on the direct correspondence between the pixels of the image and the regions of the object. Hence, the surface must be parallel to the plane of observation and it is desirable to have a speckling pattern on the surface [28]. The basic components of a DIC setup are an image acquisition system (namely a digital photographic camera), a data acquisition system (e.g., a computer) and a set of supports and lights for holding a stable illumination and the positions of the camera and the observed sample.

The images are transformed into a numeric matrix in which each pixel represents a level of light perceived by the digital sensor. The range is based on an 8-bits value between 0 and 255 in a grayscale, where 0 corresponds to pure black and 255 is pure white. Each pixel is also associated to a local field (pattern) that permits to observe individual changes and deformations, as well as translations on the observed regions The images permit to build maps for describing the local behaviour of entire surfaces, such as strain fields, strain vectors and micro cracks [29]. As shown in Fig. 1, the identification of regions and their corresponding control points permit to assess the relative displacement of the regions as well as the deformation of the subsets, which permits stablishing a series of virtual extensometers (referred to specific points) as well as obtaining generalised maps for following deformations on the entire analysed surface.

The analysis software correlates the displaced patterns with discrete functions based on the cartesian plane. The measurements obtained by the means of the DIC technique may have resolutions of the order of 10^{-9} up to 10^2 m, with acquisition rates up to 200 MHz [30]. The frequency and the length of the experiment must be coherent with the observed phenomena. One of the most important challenges associated to the DIC technique lies on the selection of the contrasting pattern. It must not significantly interfere with the studied phenomena. Furthermore, it is desirable to have isotropic and high contrasting patters, avoiding repetitive patterns. Of course, the pattern must not present visual alterations during the observation period.

3. Materials and methodology

The aforementioned DIC approach was used to characterize the superficial short-term shrinkage of different LC-TRM solutions tested under the framework of project SafEarth (Seismic Protection of Earthen Constructions) [23]. The project considered a series of tasks devoted to the characterisation of the LC-TRM solutions, namely based on their components (the mortars and the textile reinforcements) and the interaction with the substrate [7]. In this context, the solutions characterised within the experimental program presented here resulted from the combination of three different mortars with two different meshes, while considering the reference condition of a coating without reinforcing mesh. Thus, nine different samples were monitored with DIC. The subsequent sections describe the materials used in the experimental program, the preliminary trials conducted for calibration of the method and the testing methodology followed for the subsequent tests. The mechanical characterisation of the LC-TRM composite systems was not performed during these experimental campaigns. Nevertheless, the work of Barroso [23] and Romanazzi [24] extensively reports the mechanical characterisation and retrofitting impact of the LC-TRM systems herein used.

Table 2
Shrinkage and mechanical properties under the influence of water (W) and sand content (S) of 40x40x160mm samples of different earth mixtures, as displayed in Ruzicka et al. [27].

| Sample	Mixture	Density [kg/m^3]	Linear shrinkage at 28 days [mm/m]	Compressive strength [N/mm^2]
Water content:				
C_W8	8 % water	2138	17.74	8.94
C_W10	10 % water	2189	22.55	10.63
C_W12	12 % water	2163	32.48	8.77
C_W15	15 % water	1945	51.11	5.81
C_W20	20 % water	1946	67.23	6.10
Sand stabilisation (water content 10 %)				
C_S10/ W10	10 % sand	2152	18.82	7.88
C_S20/ W10	20 % sand	2164	13.19	6.84
C_S30/ W10	30 % sand	2164	7.03	6.22
C_S40/ W10	40 % sand	2141	4.52	4.75
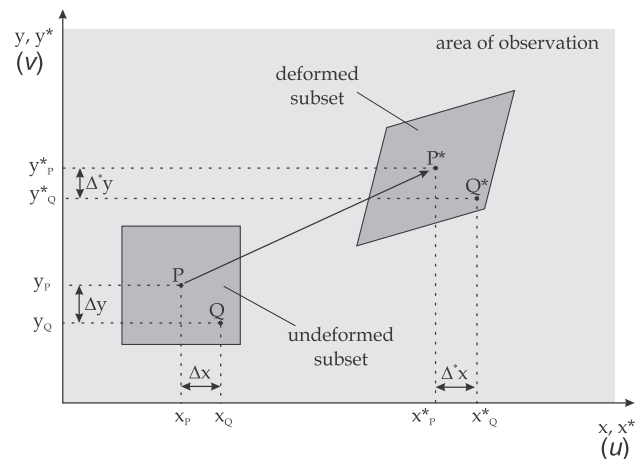
Fig. 1. Description of the displacement field of a subset in the observation area (adapted from [29]).

3.1. Materials

The experimental program considered the assessment of LC-TRM solutions resulting from nine combinations of different mortars (three) and reinforcement conditions (three).

It should be noted that the mortars and the meshes were previously characterised in Barroso [5]. The mortars consist of an unstabilised earth-based mortar (EM2.0), an earth-based mortar stabilised with hydraulic lime (S20EM2.0) and a cement-lime-based mortar (CHM). Despite this last mortar not being deemed as compatible with earthen supports, its consideration aimed at evaluating the shrinkage behaviour in case mortars conventionally used for plastering modern brick masonry walls are applied to rammed earth. Furthermore, mortar S20EM2.0 was originated from mortar EM2.0 by incorporating 20 % of hydraulic lime. Each combination received a specific key for the experimental program as summarised in Table 3, combining the type of plaster (PE for Soil and Sand, PEL for Soil, Sand and Lime and PEC for Cement, Sand and Lime) and the reinforcement condition (U for Unreinforced, G2 for the Glass Fibre mesh and G8 for the Nylon mesh).

The proportions (in wt.%) of the raw materials composing of the mortars, the water/solid (W/S) ratio and the properties are presented in Table 4, where *LS* is the linear shrinkage, f_c the compressive strength, f_b the flexural strength and the Young's modulus (E) at 28 days of age. It should be noted that all mortars were defined with similar workability, namely a flow table value of about 170 mm. The water/solid ratio is based on the suggestions of Gomes [25], based on optimal workability conditions when a flow table value of 170 mm is achieved. The contraintuitive increase of the Young's modulus for the lime-stabilised mortar may be explained by the relatively slow hardening process of this type of binder.

The reinforcement conditions considered first the reference case, where no reinforcing mesh is included, and then two situations of reinforcement with different synthetic meshes, widely available in Portugal: a common glass-fibre (G2) and a nylon (G8) mesh. The glass-fibre mesh has the larger tensile strength and stiffness, while the nylon one is more flexible and has a larger deformability. The properties obtained during the experimental campaigns of Barroso [23] for the meshes are summarised in Table 5. The linear density of the fibres is given in the international system TEX, that determines (for each direction X, Y) a ratio between mass in grams (M_S) and the length in kilometres (L) of the fibre. The grammage of the mesh by direction ($g_{x, y}$) is the ratio between the TEX indicator and the separation between the fibres in a determined direction in millimetres (Δ_D). The possible combinations of mortars and reinforcements defined nine experimental samples, as shown in Table 3.

3.2. Preliminary calibration of the shrinkage tests

Preliminary tests were conducted to better understand the potential challenges during the DIC implementation, by permitting to assess the most suitable conditions for the subsequent experiment with respect to the required speckle pattern. Three calibration trials considered coating surfaces with 20x20cm^2 of area and 1 cm of thickness of the earth-based mortar EM2.0. The first 2 trials were applied on the surface of a rammed earth wallet with dimensions 550 × 550 × 200 mm^3. The wallet was built within the framework of project SafEarth and was constituted by 9

compacted layers, being the soil mixture constituted by 14 % of clay, 16 % of silt, 32 % of sand and 37 % of gravel [31]. The surface was previously cleaned before each application. Firstly, the loose particles were scrapped with a steel brush and then a nylon one was used for eliminating remaining dust.

This calibration test was performed in absence of natural light, by using a LED lamp fixed to a support as the only light source. The sensor for this and all subsequent tests was a Nikon D800E with a 24–120 mm lens, permitting to reach a resolution of 36,3 megapixel. The shooting control and image storage relied on its connection to a computer. The pictures were captured in a time frame of 10 s with an aperture setting of f/6.3 and shutter speed of 1/60 s. The DIC analyses were performed by using GOM Correlate [32] and MatLab Software [33].

To facilitate the application of the mortar, a timber square-frame was fixed to the wallet and the surface was sprayed with water to reduce the absorption from the mortar. The mortar was applied in one layer and smoothed. Immediately after, the different speckle patterns tested in each trial were applied. The first trial included the application of earth dust by blowing, in order to mitigate the light reflection caused by the presence of mixing water of the mortar at the surface. Then, white and black paintings were sprayed in order to create the pattern. Nevertheless, the surface was not completely covered with paint, since this could affect the evaporation and drying process. A visible homogeneous and balanced pattern of earth, black and white points was preferred instead.

The observations were developed along two hours with a lapse of 30 s between photographs (Fig. 2). The analysis of the images permitted to recognise that the brightness of the humid surface in the initial stages of the observations was still problematic. Furthermore, the creation of the pattern was difficult and consumed more than 4 min, which did not permit to take images of the early stages of the drying process.

The second trial consisted in repeating the procedure of the first trial, but white limestone powder was blown against the surface, instead of black and white spray paint, to create the speckle pattern. The vertical orientation of the wallet was found to be a problem for the correct application of the powder, which accumulated in some regions leading to photos with unsatisfactory quality for DIC. As a result, the third trial considered a smaller support element in horizontal orientation. For the sake of simplicity, the support element was constituted by two fired-clay bricks placed side by side. For this trial, the limestone powder was applied by means of a sieve (Fig. 3). Furthermore, the trial test was conducted in a room with very good natural lighting conditions. The images obtained along two hours of observation were considered satisfactory, since the pattern was adequately uniform and presented the quality for measuring deformations, while its application time was inferior to 1 min.

3.3. Rammed earth specimens

Since the third trial presented the best results, the experimental program proceeded with the replication of the corresponding testing setup. Thus, nine rammed earth prisms with dimensions 200 × 200 × 100 mm^3 were manufactured using the same soil mixture of the rammed earth wallet used in the calibration trials, which is constituted by 14 % of clay, 16 % of silt, 32 % of sand and 37 % of gravel. The moisture content of the mixture was controlled by means of the drop-ball test [17]. Then, the mixture was compacted inside a timber mould in layers with initial thickness of 10 cm, which resulted in a compacted thickness of about 6.5 cm and a total of 3 layers per specimen. The layers were compacted with a steel hand rammer and the specimens were demoulded immediately after compaction. Two hours after, the specimens were stored in a climatic chamber with controlled conditions of 20 °C ± 1 °C of temperature and 60 % of relative humidity. An average density of 2050 kg/m^3 was obtained after the drying of the specimens in these conditions for a period of 28 days (Fig. 4).

Table 3
Matrix of samples based on the combination of the different mortars and reinforcement conditions.

Reinforcement condition	Mortar		
	EM2.0	S20EM2.0	CHM
No reinforcement	PE-U	PEL-U	PEC-U
Nylon mesh (G8)	PE-G8	PEL-G8	PEC-G8
Glass-fibre mesh (G2)	PE-G2	PEL-G2	PEC-G2

Table 4

Proportions and properties of the mortars adopted in the experimental program of Barroso [23].

Mortar	Cement [%]	Hydraulic lime [%]	Soil [%]	Sand [%]	W/S	LS [%]	f_c [MPa]	f_b [MPa]	E [MPa]
EM2.0	–	–	33	67	0.17	0.7	0.8	0.5	3431
S20EM2.0	–	18	27	55	0.21	1.1	1.0	0.7	1484
CHM	9	4	–	87	0.17	0	2.0	1.6	4992

Table 5

Mechanical properties of the meshes used in the experimental program (adapted from [23]).

Mesh	G2 (glass-fibre)		G8 (nylon)	
Direction	X	Y	X	Y
Threads separation (mm)	8	9	16	21
TEX = M_S/L	471	424	765	874
g = TEX/Δ_D	52.3	53.0	36.4	54.6
Tensile strength (kN/m)	16.8	12.2	2.4	4.3
Maximum strain (mm/m)	≥20	≥16	≥600	≥540
Modulus of elasticity (kN/m)	980	626	14	19
Cost (€/m2)	0.85		0.63	

3.4. Testing procedure of the shrinkage tests

The same testing procedure was repeated for all conducted tests, which was based on the procedure followed in the third calibration trial. Firstly, all the elements were positioned, namely the camera was fixed and the rammed earth specimen was placed in its definitive position, which allowed to calibrate and focus the camera. Before the application of the mortar, the surface of the prism was brushed with a nylon brush and subsequently sprayed with water. A timber frame was fixed to the prism to facilitate the application of the mortar in terms of thickness control. Then, the mortar was applied in a single 10 mm layer when the solution being tested did not include reinforcement. When it included reinforcement, a first layer of mortar of about 5 mm of thickness was
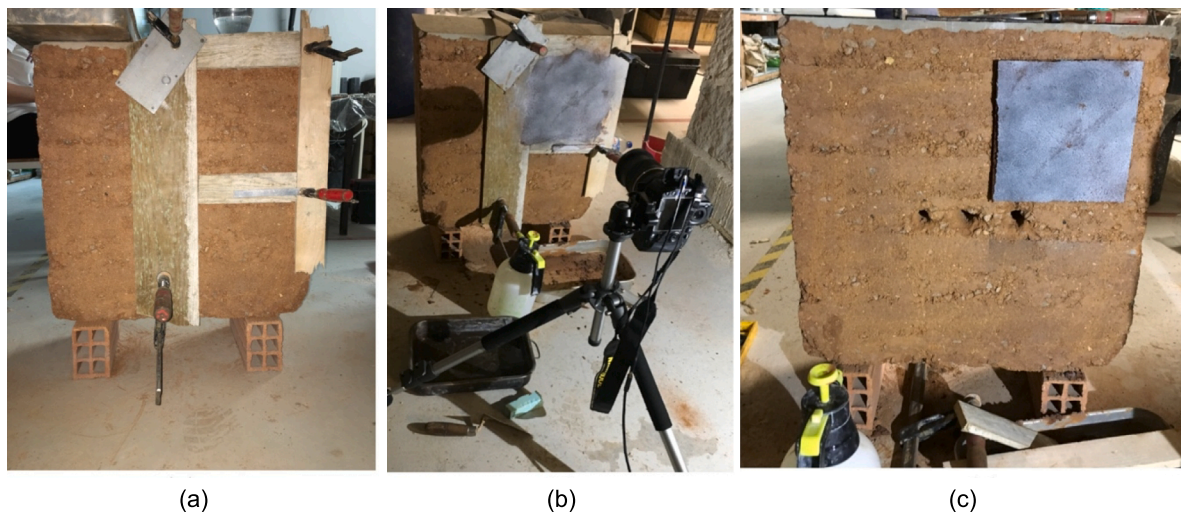

(a)   (b)   (c)

Fig. 2. Preliminary calibration tests conducted on a rammed earth wallet: (a) timber frame for applying the mortar; (b) testing setup; (c) speckle pattern of the first trial.

(a)   (b)

Fig. 3. Third preliminary calibration trial: (a) application of the limestone powder (b) testing setup.
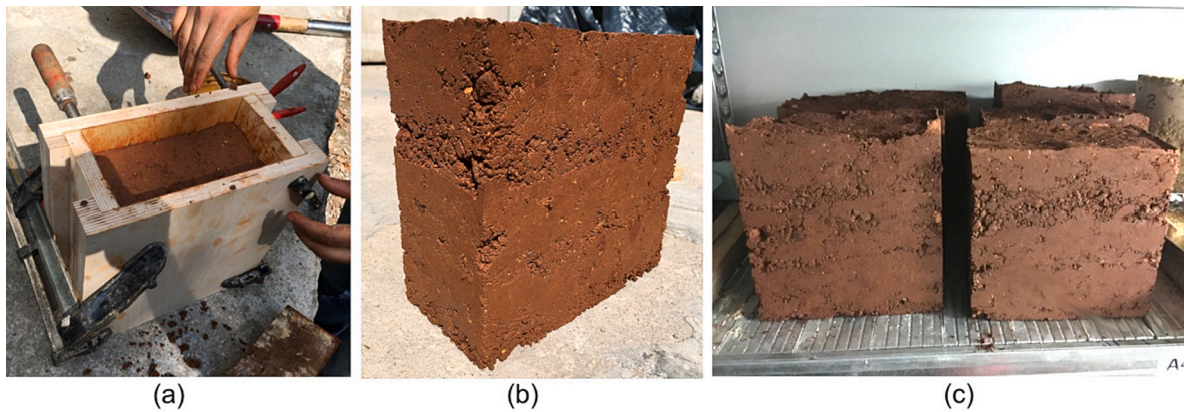
Fig. 4. Manufacturing of the rammed earth prisms: (a) timber formwork; (b) specimen immediately after demolding; (c) storing of the specimens in the climatic chamber.

applied in order to receive the mesh and, immediately after, a second layer was applied until the total thickness of 10 mm was obtained.

The surface of the mortar was smoothed with a trowel before applying the speckle pattern, which consisted in spreading a small amount of limestone powder on the surface with a sieve with aperture 0.149 mm. The test started immediately after, with the acquisition of images during about 200 min with a sampling period of 30 s (Fig. 5). Despite all concerns had in the preparation and execution of the tests, some difficulties were still observed, such as minor changes in natural lighting conditions through time or sightly colour changes during the drying process. However, they did not compromise the data acquisition process and subsequent analysis. Furthermore, all tests were conducted under similar laboratory environmental conditions, namely temperature of $23 \pm 2\,°C$ and relative humidity of $60 \pm 10\,\%$.

3.5. Testing procedure of the bond tests

The bond adhesion between the substrate and the LC-TRM system was assessed by using pull-off tests. As defined in the EN 1015-12 standard [34], these tests consist on applying a perpendicular tensile strength on a section of hardened mortar (previously isolated by using a core drilling machine) until sufficient isolation from substrate is reached. Nevertheless, Barroso [23] pointed out that the standard drilling procedure may induce damage on the samples, given the inherent fragility of materials. Thus, the isolation of the cores was made by a series of linear cuts in an octagonal configuration, based on the suggestions of Cardani et al. [35].

All the specimens were tested after the DIC experimental program was concluded, implying a drying process of more than 28 days. The cuts for isolating the cores were performed with a circular manual saw respecting an internal circumference with a diameter of 50 mm. The cutting reached a minimum depth beyond the substrate-mortar interface. Despite each specimen would be originally suitable for isolating four cores, the manipulation of the sample (in some cases) provoked a detachment of the plastered surface. Thus, the isolation of the cores was performed in two phases: the cores corresponding to a diagonal were firstly isolated and tested. Then, the process was repeated on the other two cores. The surface of the cores was cleaned, and the steel plates were glued to it by using an epoxy adhesive that, given its consistency, permitted a satisfactory adjustment. The tests were performed after a 30-minute period after the application of the glue in order to guarantee its correct hardening (Fig. 6).

The tests were carried-out with a servocontrolled actuator in which the load was monotonically applied, with a displacement-based control of 1 μm/s, similar to the procedure reported by Luso [36]. The specimens were fixed to a rigid frame and the testing plates were fixed to the actuator, keeping a vertical configuration. The loads were monitored by using a load cell with a capacity of 10 kN, while the strain was registered
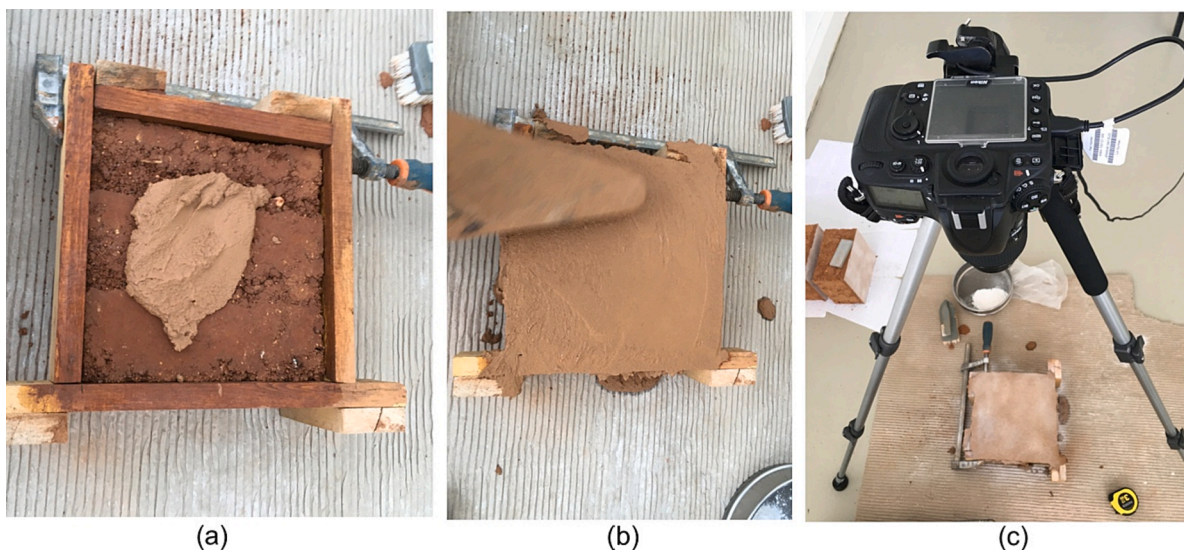

Fig. 5. Execution of the DIC shrinkage tests (PE-U specimen): (a) application of the mortar with the substrate previously moistened; (b) smoothing of the mortar; (c) testing setup.

Fig. 6. Preparation of the specimens for the pull-off tests: (a) process used for isolating the cores with octahedral shape.; (b) bonding of the steel plates with epoxy resin.

with three LVDT (Lineal Variable Differential Transformers) radially distributed (Fig. 7).

4. Results and discussion

4.1. Shrinkage behaviour

For sake of simplicity, the results were first analysed by considering a set of digital extensometers located on the surface of each specimen, as illustrated in Fig. 8. Virtual Extensometer 1 (E.V.1) corresponds to the line between points 1a-1b, with a total initial length of 28.3 cm that correspond to the maximum diagonal of the surface. Extensometers E. V.2 and E.V.4 correspond to a cross of the X and Y axis passing through the geometrical centre of the surface, having a length of 19.0 cm. The control points are located 0.5 cm from the boundary between the mortar and the formwork in order to avoid any potential effect caused by this last element, mostly given the volumetric variations of the wooden formwork due to the water absorption. Extensometers V.E.3 and V.E.5 are situated on the axes as well, but with a centred length of 9.5 cm. Behavioural differences between extensometer pairs E.V.2–E.V.4 and E.
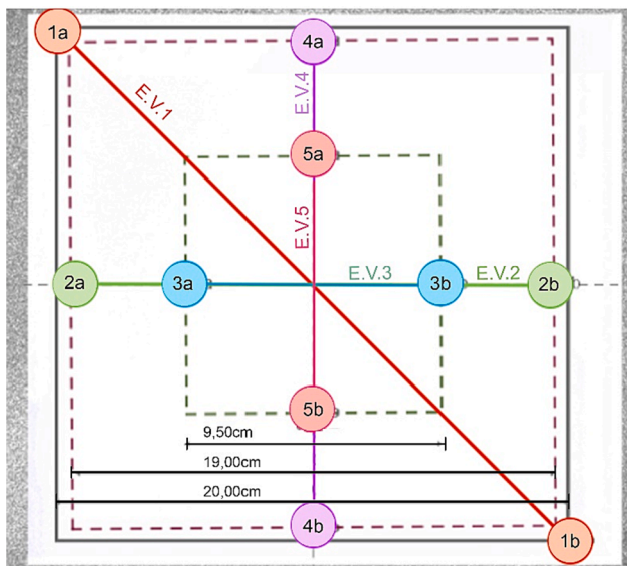

Fig. 7. Testing setup of the pull-off tests.

Fig. 8. Position of the digital extensometers considered for the analysis of the results.

V.3–E.V.5 would be meaningful for reflecting boundary-related effects.

Plotting the deformation values obtained for each digital extensometer against time allows to observe the evolution of the shrinkage during the period of observation. Fig. 9 presents the curves of the three specimens that used the earth-based mortar EM2.0, where a significant difference in deformation can be observed from the unreinforced to the reinforced specimens. This difference is especially notorious for extensometers 1, 2 and 4, which are the longest ones and have measuring points located near the borders of the specimens. On the other hand, the extensometers 3 and 5 present near zero values for all specimens. Such behaviour seems to reflect that shrinkage at the central region is more constrained than at the borders of the specimen, probably due to the lack of continuity. Hence, this effect at the borders could be strongly related to the scale of the specimens.

The unreinforced EM2.0 mortar presented high deformations, in the order of 0.7 mm, while the reinforced solutions of the same mortar exhibited a maximum value of 0.25 mm. The glass-fibre mesh reinforcement presents higher dispersion of deformations than the nylon mesh reinforcement. It should be noted that the observation of some peaks during the measurements can be associated to specific artifacts of lighting variation, yet such perturbations do not compromise the observed long-term tendencies. Observations of the PE-G8 specimen were interrupted after 120 min, given a perturbation on the light conditions that forced to stop the experiment.

Despite the relevant shrinkage deformations of the unreinforced mortar EM2.0, no visible cracks were observed after complete drying, which can be attributed to the capacity of the mortar to accommodate such deformations during the hardening, due to the typically high plasticity found in earth-based mortars. However, the presence of the meshes is shown to produce a significant reduction of the shrinkage deformations of the mortar.

Fig. 10 presents the shrinkage deformation curves of the three specimens tested with the stabilised earth-based mortar S20EM2.0, where the tendencies seem similar to those of the previous set of specimens, yet they reflect the impact of the use of hydraulic lime in limiting the volumetric changes of the clay particles. The specimen with the unreinforced mortar S20EM2.0 presents a maximum shrinkage deformation of about 0.3 mm and, as in the case of the specimens with the unreinforced mortar EM2.0, the maximum deformation is attained for the extensometers considering points near the edges of the specimens. The deformations in the central regions of all specimens with mortar S20EM2.0 are significatively less distributed than those with the EM2.0 mortar, which also reflects the volumetric stability of the S20EM2.0 mortar. Furthermore, the presence of the reinforcement meshes limits the deformations up to a maximum value of 0.1 mm. It should be noted that no cracks were visible during or after the tests of all specimens with mortar S20EM2.0. Observations on the PEL-G8 specimen stopped after 150 min due to the failure of a camera's battery, forcing the manipulation of the device.

Fig. 11 presents the shrinkage deformation curves of all specimens tested with the cement-based mortar CHM, which was observed to have the worst workability during its application. The specimen without reinforcing mesh presented a maximum deformation value of the order of 0.3 mm, while those with reinforcement presented maximum values of the order of 0.15 mm. This tendency is compatible with those observed for the precedent mortars. Observations of the PEC-G2 specimen cover only the first 150 min of the experiment, given a change in the environmental light conditions.

Nevertheless, a notable difference was observed in behaviour after the end of the DIC monitoring. The PEC-U specimen presented a crack and partial detachment of the mortar in the second day after the test (Fig. 12a). This observation suggests a weak bond between the substrate and the mortar, which is expected to be a consequence of the long-term shrinkage deformations occurring from the hardening process. Such behaviour seems to have been prevented by the presence of the reinforcement meshes in the specimens PEC-G2 and PEC-G8 specimens. The reinforcing meshes limit the shrinkage deformations of the mortar, which impedes further degradation of the bond during the hardening process.

The information obtained from the digital extensometers provides evidence of a behavioural change due to the presence of the meshes. This difference, however, is hardly observable at naked eye. Furthermore, no visible changes were observed in the weeks following the monitoring of the specimens with DIC (Fig. 12b). The results also reflect relevant differences between the three tested mortars. The solely observation of the unreinforced specimens reflects how the earth-based mortar has very high shrinkage deformations during drying, yet it seems to properly bond to the rammed earth support without cracking, thanks to a higher fresh-state plasticity. On the other hand, the stabilisation with lime seems to significatively reduce shrinkage deformations to levels comparable to the cement-based mortar. Despite the lower short-term shrinkage observed in the cement-based mortar, it was found to have limited compatibility with the rammed earth support, as long-term shrinkage resulted in cracking and detachment. No relevant differences were observed regarding the pairs of extensometers 2–4 and 3–5, suggesting that the behaviour was similar in the XX and YY directions.

The DIC monitoring also allowed to generate contour maps of the maximum principal strains, as shown in Fig. 13 for all specimens at an age of about 3 h. In general, the specimens with coatings applied with the earth-based mortars EM2.0 or S20EM2.0 generated distributed strain patterns, which contribute to dilute the shrinkage deformations through all application area, avoiding visible cracking development of these mortars, despite their high linear shrinkage. Such observation also evidences the contribution of the plastic behaviour of these earth-based mortars in avoiding cracking. Furthermore, the reinforcement of these mortars led to formation of zones around the mesh with concentration of tensile strains for both tested meshes. With respect the specimens with coatings applied with mortar CHM, a similar behaviour was observed for the unreinforced and reinforced specimens. A total absence of distribution of shrinkage deformation is observed, which may explain the lower tolerance of this mortar to accommodate long-term shrinkage deformations.

Finally, the observations conducted in all specimens evidence a different shrinkage behaviour between the central regions of the coatings and their boundaries. The contour maps of the tensile strains (see Fig. 13) also exhibit a clear cracking development at the perimetral limits of the mortar in all specimens. This observation is probably

(a)

(b)

(c)

Fig. 9. Strains by Digital Extensometer for all specimens with application of the mortar EM2.0: (a) PE-U; (b) PE-G2; (c) PE-G8.

associated to the small scale of the conducted tests, which should be an issue addressed in further investigations, where testing larger specimens would permit to assess how sensible are the results in this context. Furthermore, it is convenient to consider that the hygroscopic nature of the wood-based formwork possibly played a role during the monitoring. First, by swelling due to absorbing water from the mortar and then by shrinking due to the subsequent drying. The study of the influence of the formwork and the manipulation of specimens during the experimental program should also be further analysed in future investigations.

4.2. Bond behaviour

A total of 25 successful tests were performed. Some cores were accidentally destroyed or damaged during the cut procedure or the fixation of the actuator. This circumstance is also linked to the relative fragility of the materials. More specifically, no results were obtained from specimen PEC-U. Table 6 presents the bond strength values

obtained in each test, as well as the failed attempts. Given that all the cores exhibited failure due to detachment at the interface LC-TRM–substrate (Fig. 14), the presence of the mesh does not seem to be relevant for conditioning the bonding behaviour. Nevertheless, some material of the substrate's surface was always glued to the mortar cores, which suggest that the rammed earth at the surface has lesser cohesiveness than the inner material. This may be explained by the exposition to the environment of the surface and/or by some damage induced during the preparation of the specimens and testing setup. In fact, the most problematic stage of the experimental program was to isolate the cores trying not to induce damage to the specimens.

Despite all the values are relatively low, there is a certain better behaviour on the specimens with the PEL solution (i.e., the plaster based on a mixture of earth and lime), suggesting a more suitable compatibility with the substrate. Furthermore, this behaviour may indicate some consolidating effect on the surface of the rammed earth substrate, where part of the lime was probably absorbed to the pore structure and
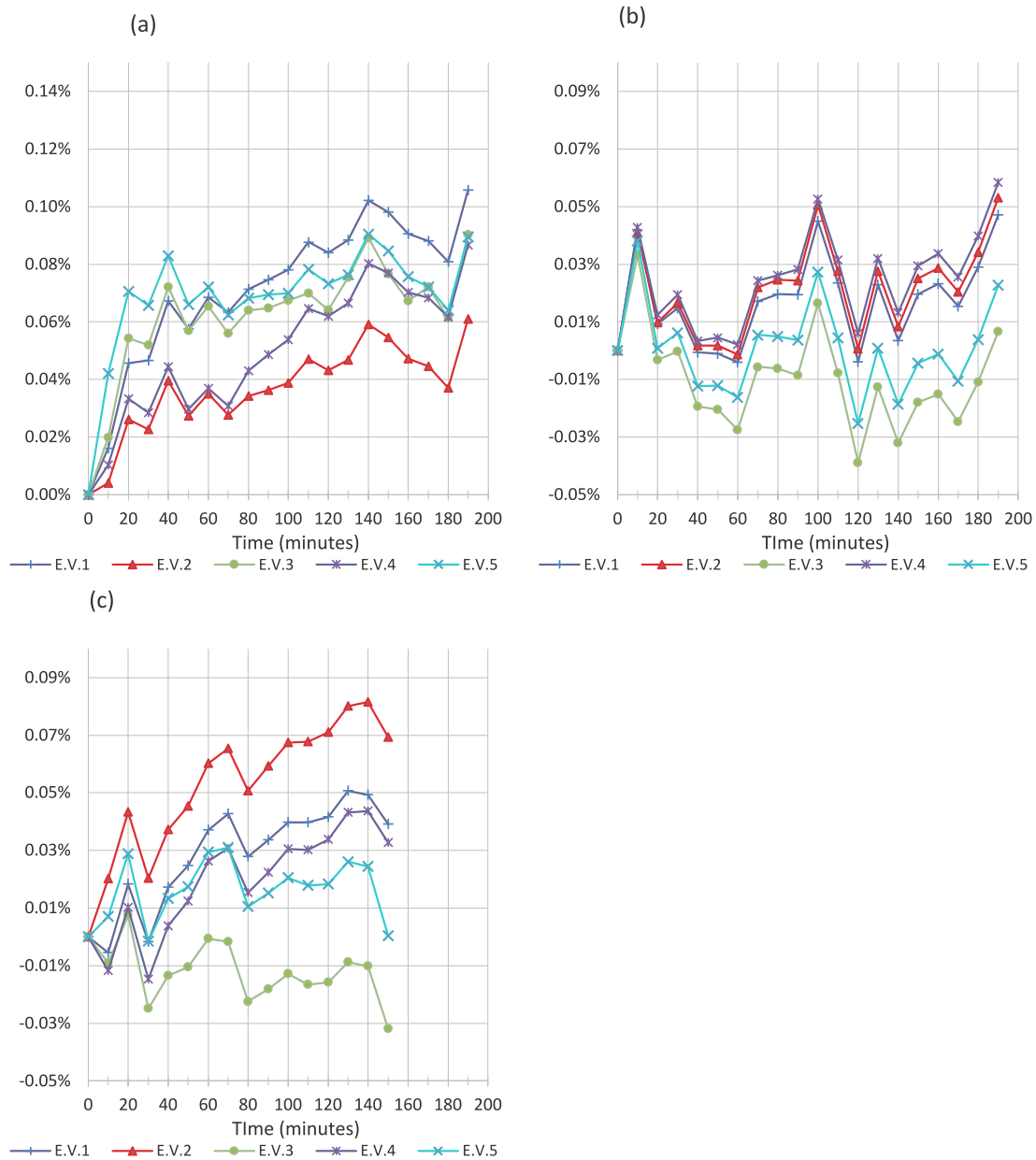
Fig. 10. Strains by Digital Extensometer for all specimens with application of the mortar S20EM2.0: (a) PEL-U; (b) PEL-G2; (c) PEL-G8.

stabilised the material. The tests performed on the PC specimens (those with a mixture of cement) were characterised by fragile failures and spontaneous detachment of large regions.

The results obtained from this experimental campaign have a large variability, which may be related to localised damage, irregularities on the surface and a variability between the mechanical properties of the rammed earth specimens. This condition limits the obtention of solid conclusions, but the overall experience represent a series of insights for enhancing and enriching future experimental programs.

5. Conclusions

Digital image correlation was shown to be suitable for monitoring the superficial shrinkage of LC-TRM systems used for the strengthening of rammed earth walls. Nevertheless, some limitations were found during the experimental program. These experiences might help to prepare improved experimental programs in the future. For instance, the use of a wooden-based formwork would have induced some border

effects due to the hygroscopic nature of the material. In future tests, it would be preferable to select a material with a minor sensitivity to water. This impact, however, is able to be assessed by the means of DIC observations, namely by using specifically devoted digital extensometers. This future work would permit to contextualise some of the observations herein presented. The control of the light was a challenging situation throughout the experimental program. Despite the tests being performed in a room appropriately illuminated, it is possible that minor changes due to natural light were meaningful for introducing variations during the tests.

The definition of the speckle pattern for monitoring the surface represented a relevant challenge. Nevertheless, the use of limestone powder revealed to be a suitable solution due to its satisfactory contrast against the natural colour of the earth-based mortar and its relatively low influence on the hardening process. The experimental setup was demonstrated to be convenient for the size and nature of the tested specimens, but it may be unsuitable for larger samples that cannot be horizontally placed. For this reason, the setup needs further
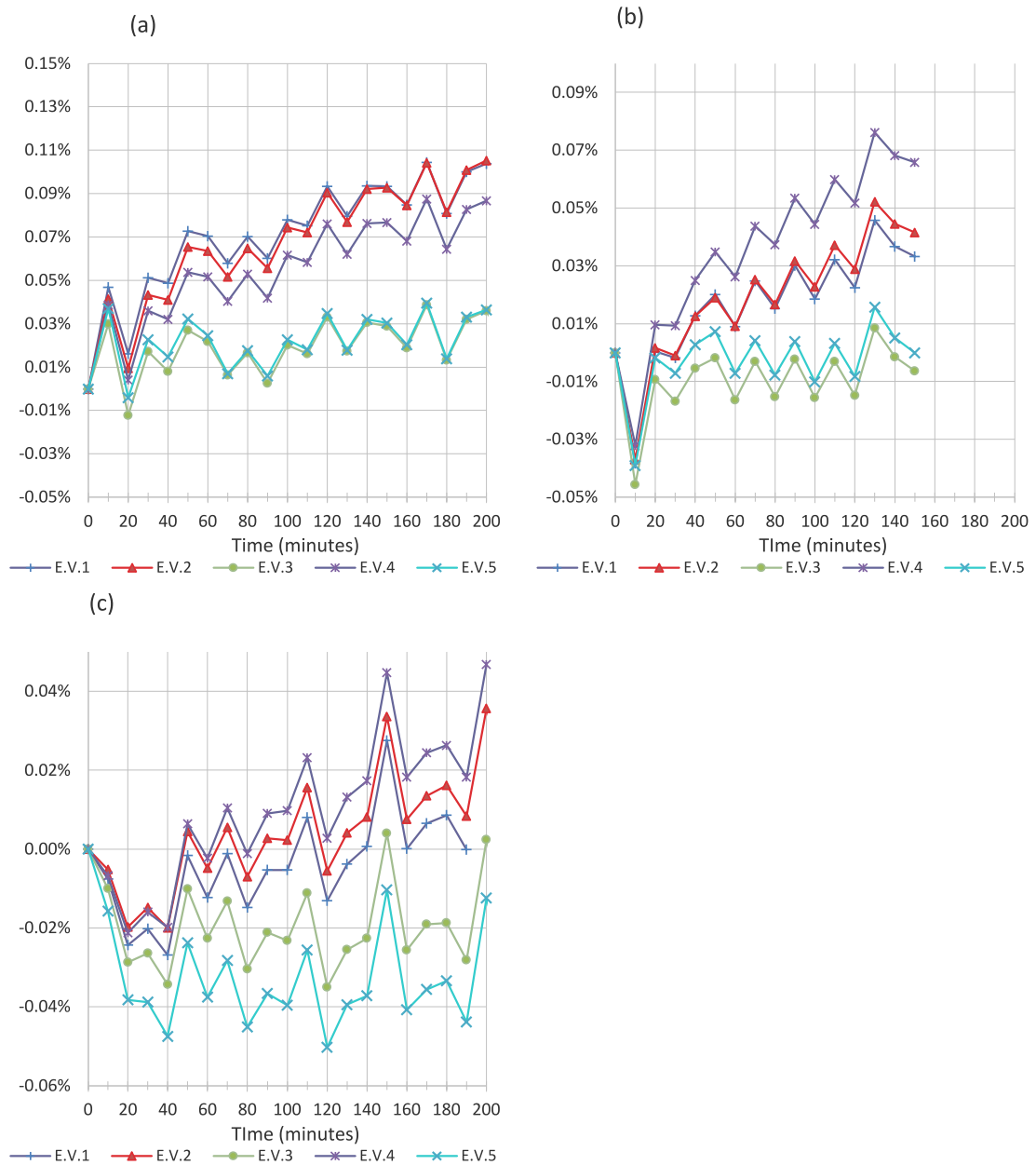
Fig. 11. Strains by Digital Extensometer for all specimens with application of the mortar CHM: (a) PEC-U; (b) PEC-G2; (c) PEC-G8.
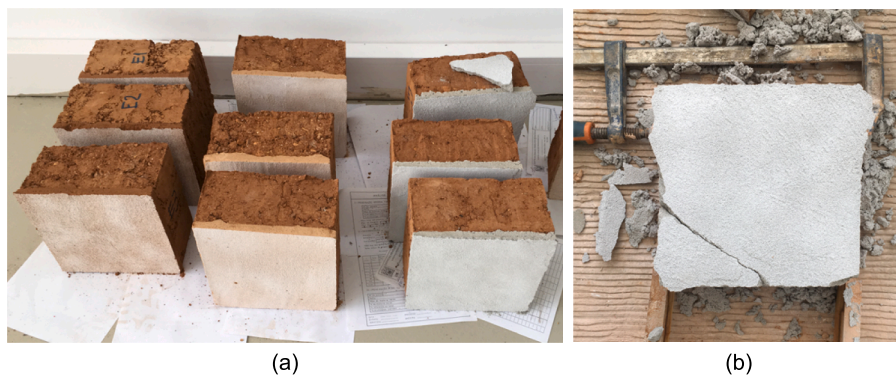

Fig. 12. Specimens after monitoring with DIC: (a) general view after 2 weeks; (b) cracking and detachment of the specimen PEC-U.
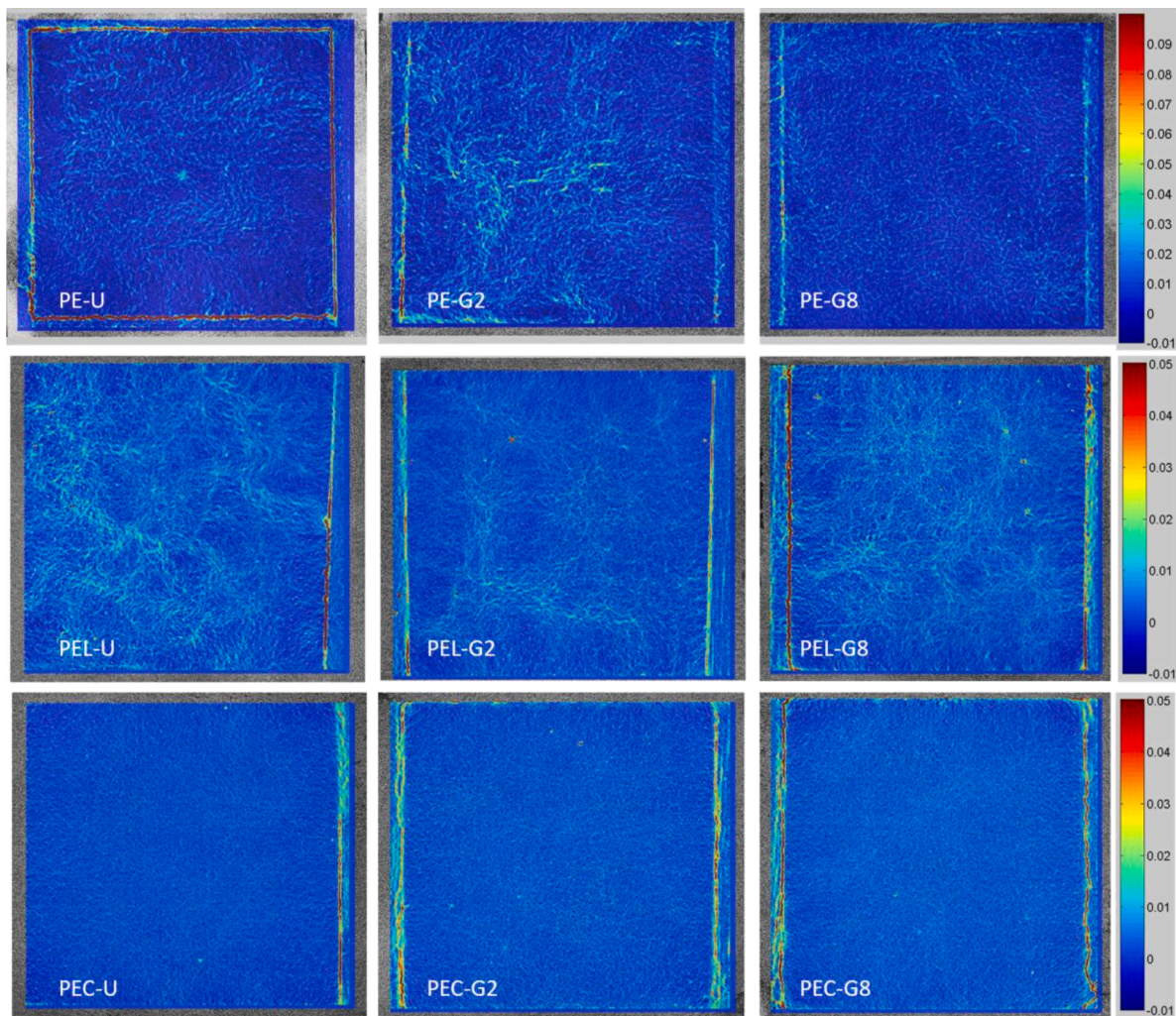
Fig. 13. Contour map of the tensile principal strains of each specimen at about 3 h of age.

Table 6
Summary of results obtained from the pull-of tests (empty cells correspond to unsuccessful tests).

Specimen	Bond adhesion strength by test (kPa)				Mean value	Coefficient of
	S_1	S_2	S_3	S_4	(kPa)	Variation
PE-U	9.17	–	1.88	–	5.53	0.93
PE-G8	7.89	16.14	20.52	–	14.85	0.43
PE-G2	37.64	–	–	–	37.64	–
PEL-U	16.76	26.89	5.04	–	16.23	0.67
PEL-G8	40.13	35.09	40.44	45.53	40.30	0.11
PEL-G2	28.47	77.41	36.36	35.09	44.33	0.50
PC-U	–	–	–	–	–	–
PC-G8	55.31	7.89	12.02	33.21	27.11	0.81
PC-G2	26.23	19.91	5.70	4.43	14.07	0.76

developments on a process to easily apply the selected speckle pattern on rammed earth walls.

The monitoring of the specimens occurred along approximately 200 min, showing a stabilising tendency in the specimens with the application of the unstabilised and lime-stabilised earth mortars. The cement-based mortar was observed to have a longer shrinkage process due to the chemical hardening process of the material, which must be considered for further analysis.

Regarding the shrinkage deformation within each specimen, it was mainly concentrated at the borders, which can be explained by the smaller restriction effects opposing to deformation. Nevertheless, a diminution of the shrinkage was observed when the meshes were integrated. This observation seems to indicate that the meshes allow a more homogeneous behaviour and strain distribution.

The unstabilised earth-based mortar (EM2.0) presented the largest shrinkage deformations, yet no visible cracks were found, which demonstrate its elevated capacity for accommodating the developed deformations. The introduction of meshes, however, represent a very important improvement of this behaviour. The unreinforced stabilised earth mortar (S20EM2.0) showed the best performance in terms of workability as well as a significative reduction of deformations when compared with EM2.0, which may indicate a loss of plasticity in the early stages of the drying. Nevertheless, the results obtained from this experimental program are not sufficient for proving this hypothesis and deserve further research. This assumption must be analysed in further works. The cement-based mortar (CHM) presented a very reduced early-age shrinkage, yet further long-term shrinkage led to cracking and partial detachment of the mortar.

The pull-off tests presented numerous challenges and difficulties related with the isolation of the cores and the fragility of the material towards its manipulation. The experimental procedure herein presented was designed and implemented as an attempt for overcoming previously identified problems. Therefore, the experimental results must be read in this context. The results are not conclusive given the high variability among them and the uncertainty associated to the experimental procedure. Nevertheless, this experience suggests that the plaster of earth stabilised with lime (S20EM2.0) has a better performance in terms of

Fig. 14. Failure modes observed in the puff-off tests: (a) example of failure at the interface LC-TRM–substrate, showing a slim superficial layer of the substrate attached to the mortar; (b) large regions of the plaster detached during the experiments.

bond strength, pointing a positive effect of superficial consolidation when stabilising the earth mortars with lime. The failure modes suggest that the presence of the reinforcement mesh does not influence the bonding behaviour. Future experiences may observe that the procedure for isolating the cores is critical for adequately perform the tests.

CRediT authorship contribution statement

Rafael Ramírez Eudave: Conceptualization, Methodology, Investigation, Data curation, Formal analysis, Visualization, Writing - original draft, Writing - review & editing. **Rui A. Silva:** Conceptualization, Methodology, Validation, Formal analysis, Investigation, Resources, Supervision, Funding acquisition, Project administration. **Eduardo Pereira:** Conceptualization, Methodology, Software, Formal analysis, Resources, Data curation, Supervision, Project administration, Visualization. **Antonio Romanazzi:** Conceptualization, Methodology, Formal analysis, Investigation, Data curation.

Declaration of Competing Interest

The authors declare the following financial interests/personal relationships which may be considered as potential competing interests: Rui Silva reports financial support was provided by Foundation for Science and Technology. Rafael Ramirez Eudave reports financial support was provided by Erasmus ELARCH Program. Antonio Romanazzi reports financial support was provided by Foundation for Science and Technology. Eduardo Pereira reports financial support was provided by Foundation for Science and Technology.

Data availability

Data will be made available on request.

References

[1] J. Vargas Neumann, M. Blondet, C. Iwaki, La Intervención Del Patrimonio Edificado En Tierra En Áreas Sísmicas Y Las Cartas De Conservación, Digit. - Rev. Digit. Arqueol. Arquit. e Artes. (2012) 53–61. https://doi.org/10.14195/2182-844x_1_6.

[2] UNESCO, Craterre, Earthen architecture in today's world, 2012.

[3] F. Jové Sandoval, D. Muñoz de la Calle, L. Pahíno Rodríguez, Ensayos de erosión hídrica sobre muros de tierra (fábrica de BTC). Método, resultados y discusión, Construcción Con Tierra. Tecnol. y Arquit. Congr. Arquit. Tierra En Cuenca Campos 2010/2011. (2011).

[4] R.A. Silva, P. Jaquin, D. V. Oliveira, T.F. Miranda, L. Schueremans, N. Cristelo, Conservation and New Construction Solutions in Rammed Earth, in: Struct. Rehabil. Old Build., 2014: pp. 77–108. https://doi.org/10.1007/978-3-642-39686-1_3.

[5] R.A. Silva, D.V. Oliveira, C. Barroso, R. Ramírez, E. Pereira, P.B. Lourenço, Investigation of the bond and shrinkage behaviour of TRM strengthening for rammed earth, Rehabend (2018) 2232–2239.

[6] G. Minke, F. Mahlke, Building with straw: design and technology of a sustainable architecture - Thirdand revised edition, 3rd ed., BIRKHAUSER VERLAG AG, Basel, 2005. http://scholar.google.com/scholar?hl=en&btnG=Search&q=intitle:Building+with+earth:design+and+technology+of+a+sustainable+architecture#1%5Cnhttp://scholar.google.com/scholar?hl=en&btnG=Search&q=intitle:Building+with+earth:+Design+and+technology+of+a+sustai.

[7] A. Romanazzi, D.V. Oliveira, R.A. Silva, Experimental investigation on the bond behavior of a compatible TRM-based solution for rammed earth heritage, Int. J. Archit. Herit. 13 (2019) 1042–1060, https://doi.org/10.1080/15583058.2019.1619881.

[8] N.H. Sadeghi, D.V. Oliveira, R.A. Silva, N. Mendes, M. Correia, H. Azizi-Bondarabadi, Experimental characterization of adobe vaults strengthened with a TRM-based compatible composite, Constr. Build. Mater. 271 (2021), 121568, https://doi.org/10.1016/j.conbuildmat.2020.121568.

[9] M. Dabaieh, Building with Rammed Earth, 2014. https://www.researchgate.net/publication/269763371_Building_with_Rammed_Earth.

[10] P. Torgal, R. Eires, S. Jalali, Construção em Terra, 1st ed., Publidisa, Guimarães, 2009. http://ecocasaportuguesa.blogspot.com/2016/06/construcao-em-terra.html.

[11] L. Taghiloha, Using rammed earth mixed with recycled aggregate as a construction material, (2013) 1–88.

[12] H. Houben, H. Guillaud, CRAterre, I.T. Publications, Earth Construction: A Comprehensive Guide, Intermediate Technology Publications, 1994. https://books.google.pt/books?id=yjVSAAAAMAAJ.

[13] S.R. Duarte, Construir com a terra. Uma proposta de intervenção no Bairro do Barruncho, Odivelas., Univ. Técnica Lisboa. (2013) 244. http://hdl.handle.net/10400.5/6943.

[14] H. Schroeder, Sustainable building with earth, Springer International Publishing, Cham (2015), https://doi.org/10.1007/978-3-319-19491-2.

[15] George Ofori, Appropriate building materials: A catalogue of potential solutions, SKAT, St. Gallen 21 (2) (1997) 270–272.

[16] EN ISO 14688, 14688-1: Geotechnical investigation and testing, Identification and classification of soil, Part 1: Identification and description, 2016.

[17] New Zealand Standard, Materials and workmanship for earth buildings - NZS4298: 1998, Wellington, 1998. www.standards.co.nz.

[18] M.F. Ashby, Renewable materials, natural materials, Mater. Environ. (2021) 267–294, https://doi.org/10.1016/b978-0-12-821521-0.00011-6.

[19] D. Lacouture, L., Bernal, C., Ortiz, J.and Valencia, Estudios de vulnerabilidad sísmica, rehabilitación y refuerzo de casas en adobe y tapia pisada, Apunt. Rev. Estud. Sobre Patrim. Cult. - J. Cult. Herit. Stud. 20 (2007) 20(2),286-303.

[20] L.E. Yamin, C.A. Phillips, J.C. Reyes, D.M. Ruiz, Seismic Behavior and Rehabilitation Alternatives for Adobe and Rammed Earth Buildings, 13 Th World Conf. Earthq. Eng. (2004) 10.

[21] A. Figueiredo, H. Varum, A. Costa, D. Silveira, C. Oliveira, Seismic retrofitting solution of an adobe masonry wall, Mater. Struct. Constr. 46 (2013) 203–219, https://doi.org/10.1617/s11527-012-9895-1.

[22] A. Mordanova, S. De Santis, G. De Felice, State-of-the-art review of out-of-plane strengthening of masonry walls with mortar-based composites, Struct. Anal. Hist. Constr. Anamn. Diagnosis, Ther. Control. - Proc. 10th Int. Conf. Struct. Anal. Hist. Constr. SAHC 2016. (2016) 337–343. https://doi.org/10.1201/9781315616995-44.

[23] C. Barroso, Reforço Sísmico Inovador de Construção de Taipa, Universidade do Minho, 2017.

[24] A. Romanazzi, Seismic Protection of Rammed Earth Heritage Based on a Compatible Strengthening Technique, University of Minho, 2021.

[25] M.I. Gomes, P. Faria, T.D. Gonçalves, Rammed earth walls repair by earth-based mortars: The adequacy to assess effectiveness, Constr. Build. Mater. 205 (2019) 213–231, https://doi.org/10.1016/j.conbuildmat.2019.01.222.

[26] P. Faria, M. Gomes, Repair mortars for rammed earth constructions, Proc. XII DBMC – 12th Int. Conf. Durab. Build. Mater. Components, Vol.2, Porto, FEUP, March 2011. (2011) 689–696. http://run.unl.pt/handle/10362/9938.

[27] J. Ruzicka, F. Havlik, J. Richter, K. Stanek, Advanced prefabricated rammed earth structures—mechanical, building physical and environmental properties, Rammed Earth Constr. - Proc. 1st Int. Conf. Rammed Earth Constr. ICREC 2015. (2015) 139–143. https://doi.org/10.1201/b18046-29.

[28] H. Schreier, J.J. Orteu, M.A. Sutton, Image correlation for shape, motion and deformation measurements: Basic concepts, theory and applications, Springer US, Boston, MA, 2009. https://doi.org/10.1007/978-0-387-78747-3.

[29] E.N.B. Pereira, Processes of Cracking in Strain Hardening in Cementitious Composites, University of Minho, 2012.

[30] V. Tiwari, M.A. Sutton, S.R. McNeill, Assessment of high speed imaging systems for 2D and 3D deformation measurements: Methodology development and validation, Exp. Mech. 47 (2007) 561–579, https://doi.org/10.1007/s11340-006-9011-y.

[31] O. Dominguez-Martínez, Preservation and repair of rammed earth constructions ., University of Minho, 2015. http://www.msc-sahc.org/upload/docs/new.docs/2015_OGonzalez.pdf.

[32] Software Digital Image Correlation, GOM Correlate version 2.0.1., (2019).

[33] Natick Massachusetts: The MathWorks Inc., MATLAB Version 9.4.0 (R2018a), (2018).

[34] European Comitee for Standardization, EN 1015-12 Method of test for mortar for masonry - Part 12: Determination of adhesive strength of hardened rendering and plastering mortars on substrates, (2016).

[35] G. Cardani, L. Binda, M.R. Valluzzi, P. Girardello, M. Panizza, E. Garbin, P. Casadei, On site composites-to-masonry bond evaluation in presence of rising damp and salt crystallization, in: Brick Block Mason. Trends, Innov. Challenges - Proc. 16th Int. Brick Block Mason. Conf. IBMAC 2016, 2016: pp. 365–372. https://doi.org/10.1201/b21889-43.

[36] E. Luso, Análise Experimental de Caldas à Base de Cal para Injeção de Alvenaria Antiga, Ph.D. Thesis, Univ. Do Minho, 2012.